Chapter 25

Characterization Techniques of Nanoparticles

Javeria Arshad[*1]

1Department of Chemistry, Government College Women University Sialkot, Pakistan
*Corresponding author: javeriaarshad777@gmail.com

ABSTRACT

This work examines numerous instrumental techniques used in the characterization of nanoparticles. The main emphasis is on X-ray diffraction (XRD), scanning electron microscopy (SEM), thermal analysis (TA), and electrochemical analysis techniques like cyclic voltammetry (CV) and electrochemical impedance spectroscopy (EIS). The principles, apparatus, and applications of each technique are described, providing insights into their utility for studying various structural, morphological, thermal, and electrochemical aspects of nanoparticles. Theoretical frameworks, equations, and experimental approaches are discussed, allowing for a thorough knowledge of the characterization procedures. This review provides academics and practitioners with essential information to guide their investigations and analysis of nanoparticle materials.

KEYWORDS
Nanoparticles, XRD, SEM, TA, Electrochemical analysis

Received: 19-Jun-2024
Revised: 15-Jul-2024
Accepted: 22-Aug-2024

A Publication of Unique Scientific Publishers

Cite this Article as: Arshad J, 2024. Characterization techniques of nanoparticles. In: Ahmed R, Khan A, Abbas RZ, Farooqi SH and Asrar R (eds), Complementary and Alternative Medicine: Nanotechnology-II. Unique Scientific Publishers, Faisalabad, Pakistan, pp: 218-226. https://doi.org/10.47278/book.CAM/2024.306

INTRODUCTION

Several techniques are used for the characterization of nanomaterials. Some of them are explained below.

X-ray diffraction (XRD)

Because X-rays are non-destructive and inert, X-ray diffraction (XRD) is a commonly used characterization technique for fundamental structural study of both crystalline and non-crystalline materials. High-tech tools like X-ray diffraction (XRD) can clearly show the atomic or molecular structural features of crystals. Von Laue observed in 1912 that crystals can diffract X-rays due to their periodic arrangement. Every crystal has a distinct diffraction pattern that aids in determining its structure. The determination of particle size, d spacing, tension, phase equilibria, and crystal orientation are among the contemporary uses for this approach (Hanawalt et al., 1938).

Principle

In X-ray scattering (XRD), the crystal lattice and the incident monochromatic X-ray beam interact. When Bragg's law's requirements are met, constructive interference is observed.

$$n\lambda = 2d\sin\theta \quad (1)$$

Where θ is the angle between the incident beam and the diffracting planes, d is the distance between the crystal's planes participating in the diffraction, and n is an integer (Dinnebier and Billinge, 2008).

The scattering of photons caused by X-rays interacting with specific atom arrangements in the crystal lattice is known as diffraction. The specific phase relationship between the dispersed photons, which can result in either constructive or destructive interference, is caused by this periodic arrangement of atoms. Diffraction beams are created when constructive interference happens and all of the scattering rays from all of the atoms are in phase. Figure 1 shows how incident rays interact with various material planes diagrammatically.

Instrumentation

Three basic components make up a conventional x-ray diffractometer: an x-ray tube, a sample holder, and an x-ray detector (Bunaciu et al., 2015). X-ray tubes are made up of two metal electrodes with a high potential between them, often between 30,000 and 50,000 volts, and an electron source (Cullity, 1956). Copper, Cr, Fe, Co, and Mo are typically utilized as anode materials in x-ray tubes, and tungsten filament is used as the cathode material. By heating the filament to produce electrons, which are then accelerated toward and struck by the anode through the application of high voltage, X-rays are produced in an evacuated glass tube. The production of x-rays that radiate in all directions occurs if the bombarding electrons possess sufficient energy to remove the electrons from the target's inner shells. Figure 2 illustrates how these x-

rays combine to generate a spectrum that includes a variety of radiations, such as Kα, Kβ, Kα1, and Kα2. The equipment primarily uses Kα radiation for analysis, although Kβ and Kα1 are electronically blocked during data processing and are blocked by filters or monochromators (Jenkins and Snyder, 1996).

The x-rays are collimated by sending them through the Soller slits in order to evaluate the specimen perfectly. Goniometers, which rotate and orient the specimen in a certain direction with respect to the x-ray beam, are a feature of X-ray diffractometers. When the collimated x-rays strike the sample, constructive interference produces a diffracted x-ray beam as long as Bragg's law is met. The entering diffracted beam is recorded by a detector, which then processes and converts it into signals that may be seen on a computer or printer.

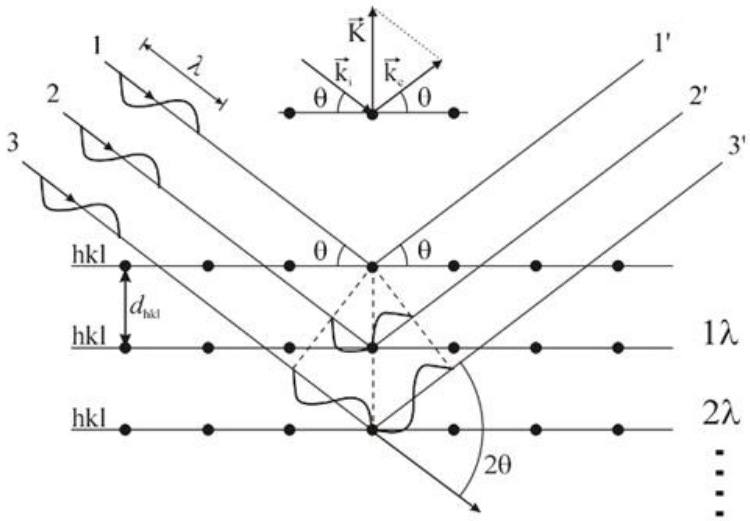

Fig. 1: The working principle of the x-ray diffraction pattern (Cullity, 1956).

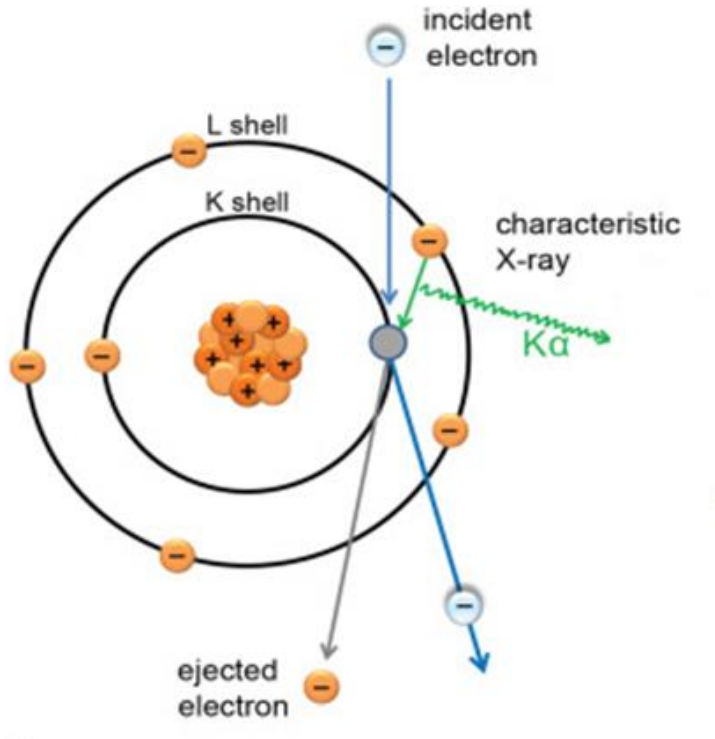

Fig. 2: Production of x-rays (Pirozzi et al., 2021).

Particle Size

When a crystal's size is less than 0.1 μm, it's referred to as "particle size" and can be determined using the Sherrer equation (Muniz et al., 2016).

$$D = \frac{57.3\,k\lambda}{\beta \cos\theta} \qquad (2)$$

λ is the wavelength of the input x-ray radiation, θ is the diffracting angle of the x-rays, and k is related to the crystallite shape. β is the broadening of the diffraction line evaluated at half its maximum intensity. According to equation 2, when

the size of a crystallite rises, the diffracted maxima's breadth (β) decreases (Alexander and Klug, 1950). The Debye-Scherrer equation is valid for the specimen with particles between 100 and 200 nm in size. It becomes difficult to determine whether the peak broadening results from crystallite size or other causes if the particle size beyond this point (Holzwarth and Gibson, 2011).

Scanning Electron Microscopy (SEM)

Using a microscope, one may discern objects that are invisible to the unaided eye. In the past, microscopes used light as the source to examine or work with the material. The resolution that is obtained is insufficient to disclose the minute details at the sub-micro and nanoscale. An electron beam is used to solve this issue since the resolution limit increases with decreasing wavelength (Hamid, 2018). Techniques like transmission electron microscopy (TEM) and scanning electron microscopy (SEM) are developed using this concept. These advanced methods provide an image with a resolution better than a light microscope by probing the specimen with an electron beam.

SEM is used to examine the topography of the surface and provide details about the bulk material's surface, near-surface, composition, and flaws. For material and biological scientists to analyze their specimens at the nano and micro levels in a variety of industries, scanning electron microscopy (SEM) is an incredibly versatile tool.

Interaction of the Electron Beam with the Specimen

An overview of the SEM's operation and equipment is shown in Figure 3. When an electron beam with energy of 2–40 keV (primary electrons) interacts with the material, it produces three types of electrons: characteristic x-rays (c), backscattered electrons (BSE), and secondary electrons (SE) (Goodhew et al., 2000).

a) Secondary Electrons (SE)

When primary electrons collide with atomic electrons and knock them out of their orbits, inelastic collision occurs, producing SE. When SE with an energy less than 50 eV escapes from the specimen's near-surface layers, a high-resolution picture is created.

b) Backscattering Electrons (BSE)

When incident electrons approach an atom's nucleus close enough to be reflected at very broad angles, they scatter, resulting in BSE. Because BSE originates from the specimen's deeper layers and has lesser energy than SE, the resulting image has poorer resolution (Vernon-Parry, 2000).

c) X-rays

Electrons from outer shells descend by releasing energy in the form of x-rays when high-energy incident electrons knock out electrons from the inner shell to fill the holes. Their resolving power is one micrometer.

Instrumentation

An electron column, a specimen chamber, a computer control system, and three components make up a standard SEM instrument. These numerous parts are designed to carry out diverse tasks related to microscopy and microchemical analysis.

a) Electron Column

An electron cannon, electron lenses, scan coils, condenser, and objective lenses make up an electron column, which is cylindrical. The cathode and related electrodes make up the electron cannon, which is situated in the highest section of the electron column. The applied potential difference causes the electron beam, which is produced by the electron cannon, to move down the electron column. Depending on the type of investigation, tungsten filament, LaB6 emitter, Schottky field emission, and cold field emission gun are the most often utilized electron sources. The electron beam that is produced is concentrated by electromagnetic lenses composed of copper coils encased in an iron shell. The focal length of electromagnetic lenses can be adjusted by adjusting the current flowing through their coils, unlike traditional lenses. A small probe size and current on the specimen come from the electron beam spreading out and being mostly blocked by the apertures as it travels through the condenser lens. Through the objective lens, the specimen's surface is the focus of the electron beam. The specimen is closely examined by two scanning electromagnetic coils inside the objective lens bore, and a signal is produced. The detectors process this signal, which consists of both BSE and SE, and an image is displayed on the screen once it has been synchronized.

b) Specimen Chamber

Specimen Chamber is positioned at the end of the electron column. A specimen chamber comprises of specimen stage, specimen holder, optional air lock chamber, CCD camera and detectors. The specimen-containing stab is inserted into the specimen stage. To obtain better signals and realign the features in the SEM image, the stage can be tilted and rotated. In order to prevent collisions, cameras play a critical role in maintaining the proper distance between the specimen

and the objective lens.

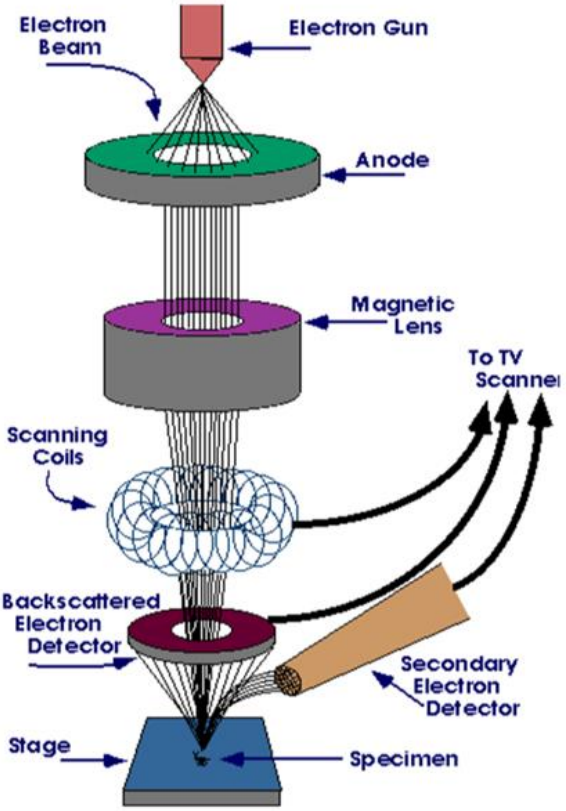

Fig. 3: The working of a scanning electron microscope (Ford et al., 2019).

c) Computer Control System

The software that comes with modern SEM devices is designed to carry out many tasks, such as data storage, networking, electron beam imaging, specimen chamber evacuation, specimen stage motions, and microchemical analysis.

Thermal Analysis (TA)

ICTAC (International Confederation for Thermal Analysis and Calorimetry) defined thermal analysis as

"Thermal analysis (TA) means the analysis of a change in a property of a sample, which is related to an imposed temperature alteration."

Thermal analysis (TA) encompasses a number of methods, including thermometry, thermomanometry, thermal gravimetric analysis (TGA), differential scanning calorimetry (DSC), and thermomechanometry. Thermal examination of a sample (usually solid) causes the atoms' lattice motion to become random at a certain temperature, which might result in one of the following phenomena: a) phase change; b) melting; c) sublimation; or d) thermal decomposition (Brown, 1989). TGA and DSC are the methods most frequently employed to examine how a specimen's thermal behavior varies as a result of temperature changes (Gabbott, 2008).

Thermogravimetric Analysis (TGA)

Using the TGA technique, variations in the specimen's mass are monitored in a controlled atmosphere at a predetermined temperature as a function of time. A thermogravimetric analyzer, sometimes known as a thermobalance, is the apparatus used to carry out the complete procedure. Two separate changes in the specimen's mass can be noticed as a result of TGA (Parlouer, 2013).

a) Weight Loss

Weight loss may happen as a result of dehydration, dihydroxylation, evaporation, decomposition, desorption, pyrolysis, etc.

b) Weight Gain

Weight gain may happen due to adsorption and hydration etc.

Instrumentation

A thermobalance houses three components: a controlled environment cabinet, a furnace, and a sensitive balance module. Although there are other varieties of thermobalance, the most often used one operates on the null position

balance concept.

a) Balance Module

A torsion wire hangs the balancing assembly, and a rod with four magnets attached goes through the middle of it. The solenoid is submerged in these magnets. A photodiode measures the signal after a light is delivered by an optical detection device. The light becomes partially obscured as soon as the sample's mass changes because the balance beam is forced to move. The solenoid receives current in order to make up for this and return the balance to the null state. The compensatory current corresponds to the variation in the specimen's mass.

b) Furnace

Certain constructional measures must be in place between the balance and the furnace to shield it from the damaging effects of heat radiation and the entrance of corrosive breakdown products (Ebnesajjad, 2010). The heating elements utilized in the majority of furnaces were nickel chrome, kanthal, platinum, and tungsten. The specimen is set atop a crucible that, even at extremely high temperatures, ought to be inert. For research conducted at higher temperatures, crucibles composed of alumina, platinum, tungsten, and graphite are utilized (Parlouer, 2013). The sample should be between 5 and 20 mg in amount, and the heating rate should be adjusted so that the specimen has enough time to finish the reactions.

c) Atmosphere

Different kinds of analyses are conducted in different kinds of contexts. Depending on the experimental conditions, some investigations require an inert atmosphere, while others require an oxidative or reductive atmosphere.

Differential Scanning Calorimetry (DSC)

Differential Scanning Calorimetry (DSC) is a technique for measuring heat flux (thermal power) to and from a specimen over time or temperature changes in a given environment. It entails comparing the heat flux of the reference crucible to the crucible containing the specimen (Gallagher, 1998). DSC permits the detection of phase changes that occur within the specimen during the heat treatment process. The approach falls into two groups based on its mechanism: heat flux DSC and power compensated DSC (Zhao et al., 2005).

a) Heat Flux DSC

A thermoelectric disk is used to support both an empty reference pan and a pan carrying specimens during the heat flux treatment process. The entire assembly is housed inside a single furnace, and a thermoelectric disk transfers heat to the pans. The temperature differential between the sample and reference pans is caused by the thermal events that take place in the specimen. Temperature sensors are made using area thermocouples (Gill et al., 2010). This temperature differential, or Δt, is measured, transformed into the equivalent of heat flow, and then recorded as a function of temperature or time.

b) Power Compensated DSC

The reference pan and the specimen pans in power compensated DSC are heated by two different heaters in two different furnaces. The reference pan and the specimen pan need to be maintained at the same temperature. Power compensation is performed to a specific furnace in the event that there is any apparent temperature change (Gabbott, 2008). comparing the energy input differences to the two furnaces and then recording the data as a function of temperature or time.

There would be a temperature differential between the reference and sample pans when the specimen underwent the heat treatment. If the specimen absorbs or releases excess heat in relation to the reference pan while maintaining the same temperature in both pans, the process is referred to as endothermic or exothermic, respectively (Gill et al., 2010).

The pan or crucible's composition should prevent it from reacting with the sample and solidifying its encapsulation. To prevent spills, the sample should be very small, ranging from 1 to 10 mg. Typically, an inert gas is present during the process; however, depending on the application, air or oxygen may be purged and utilized as oxidative agents. The gas flow is managed by restrictors and pressure regulators (Gabbott, 2008).

Electrochemical Analysis

The electrochemical analysis of the as-synthesized materials has been done by using following techniques

1) Cyclic Voltammetry (CV)

In the past ten years, cyclic voltammetry has emerged as the most well-known method for researching electrochemical reactions. It is a helpful technique to determine the energy levels of the analyte, electron transfer processes, and the thermodynamics of a redox reaction. It is the most effective technique in all electrochemical studies because of its broad application. Furthermore, the rate constant (k^), the number of electrons throughout an electron transfer process, and the thermodynamics and heterogeneous kinetics of the electron transfer reaction can all be inferred from the CV results. CV employs a three-electrode system, which comprises of a working electrode (WE), reference electrode (RE), and counter electrode (CE), just like all other electrochemical processes. Starting with an initial value, the voltage delivered to the WE in

relation to RE is scanned linearly vs time. After reaching a particular potential, the potential scan is reversed, and a counter electrode is used to monitor the current. A cyclic voltammogram is the plot of current and applied potential that results from this process (Isaev et al., 2018). Figure 4 provides a general representation of a voltammogram.

Categorization of Redox Processes

Cyclic voltammetry can be categorized into reversible, irreversible and quasi reversible processes. This classification is based on parameters like cathodic and anodic peak currents (I_{pc} and I_{pa}) and peak potentials (E_{pc} and E_{pa}), peak width (E_p-$E_{p/2}$), and half wave potential ($E_{½}$).

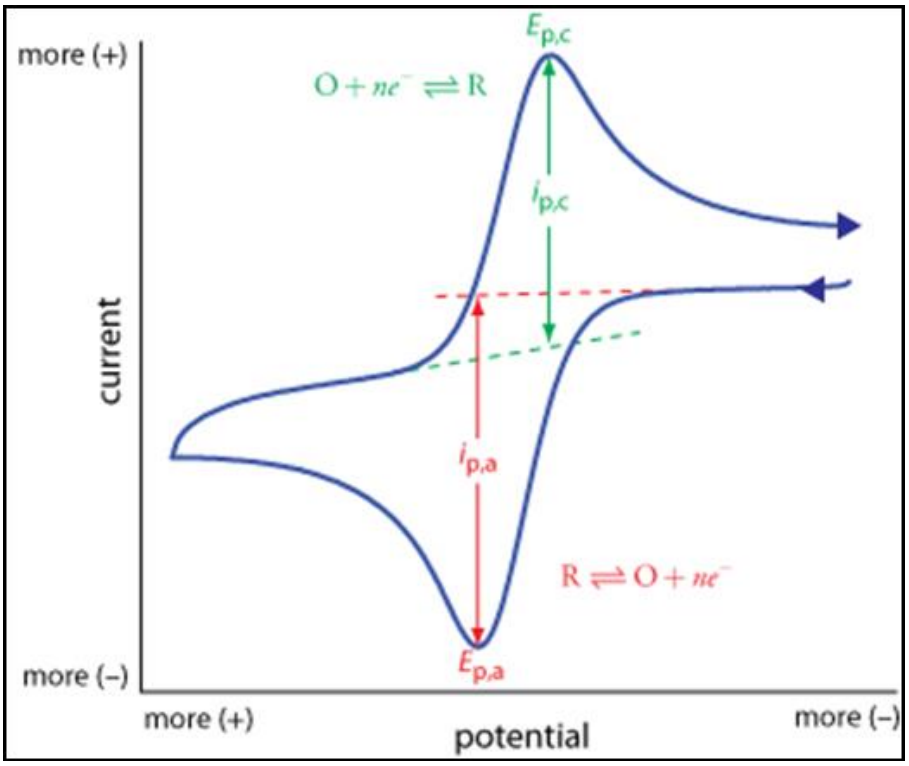

Fig. 4: Typical cyclic voltammogram featuring cathodic and anodic peaks for a reversible process (Isaev et al., 2018).

a) **Reversible Process**

The peak potential of this kind of electrochemical process is independent of the scan rate, and the forward and backward current ratio is unity. An irreversible process's peak current can be calculated using the Randles-Sevcik equation (Isaev et al., 2018). The following is the mathematical relationship:

$$I_p = (2.69 \times 10^5)\, n^{3/2}\, A\, C\, D^{1/2}\, \upsilon^{1/2} \qquad (3)$$

According to this equation I_p stands for current in amperes, n for number of electrons, A for area of the electrode in cm^2, C for concentration of the analyte in mol cm^{-3}, D for diffusion coefficient in $cm^2\ s^{-1}$ and υ for scan rate in V/s.

During a reversible process, the exchange of electrons at the electrode/electrolyte interface is often very fast. Equation 4 is used to calculate the number of electrons taking part in a chemical reaction that proceeds through a reversible process.

$$\Delta E_p = E_{pa} - E_{pc} = (0.059/n)\ V \qquad (4)$$

In reversible processes, potentials corresponding to cathodic and anodic peaks do not change with scan rate. In that situation half-wave potential ($E_{p/2}$) is used, and calculated by the following equation.

$$E_{p1/2} = E_{1/2} \pm 28/n\ (mV) \text{ at } 298\ K \qquad (5)$$

$E_{1/2}$ is that potential at which the current becomes half (I_p=0.5I_p). The positive sign signifies the oxidation process and the negative sign corresponds to the reduction process. Oxidation and reduction processes are represented by positive and negative signs, respectively. Equation 6 is used to calculate the peak potential (Isaev et al, 2018).

$$E_p = E_{1/2} - [1.109 \pm 0.002]\ RT / nF \qquad (6)$$

For a reversible process, the value of the k˚ is ≥ 2×10^{-2} cm s^{-1}.

b) **Irreversible Process**

Because of the slow electron transport in an irreversible process, the peaks are widely apart, and the peak separation is always larger than 59/n mV (Zahn et al., 2012). Moreover, the scan rate affects peak potential. For this procedure, the peak current is shown as:

$$I_p = (2.99 \times 10^5)\, n^{3/2}\, \alpha^{1/2}\, A\, C\, D^{1/2}\, \upsilon^{1/2} \qquad (7)$$

The transfer coefficient, denoted by α in this equation, quantifies the energy symmetry of electron transfer and has a

value between 0 and 1. The following relationship connects peak separation to the electron count:

$$n = 4\ I_p\ RT/\ FQ\ \upsilon \quad (8)$$

c) Quasi-reversible Process

This process sometimes referred to as the quasi-reversible process, lies between the reversible and irreversible processes. A reverse scan of this system reveals the presence of a peak. Less magnitude is seen in the forward scan, though. Peak separation in this procedure increases as the scan rate increases, and it should be greater than 60 mV. Peak potentials are widely separated in voltage micrographs.

k° values for this process ranges from 2×10^{-2} cm s^{-1} to 3×10^{-4} cm s^{-1} (Birke et al., 1981).

2) Electrochemical impedance spectroscopy (EIS)

The sum of all the resistances present in a system is collectively known as impedance. Traditional electrochemical analysis fails to fully explain the process occurring at the electrode-electrolyte interface. Impedance measurements over a wide frequency range are required for a full description of the redox reactions (Choi et al, 2020). In impedance, a small perturbed potential (V_ω) is employed to record the resulting current (I_ω). The Z_ω denotes impedance and is determined by using the following relation:

$$Z_\omega = V_\omega/I_\omega = Z_o \exp(i\phi) = Z_o(\cos\phi + i\sin\phi) \quad (9)$$

Where ω is the angular frequency, ϕ is the phase angle, i is the imaginary unit, V_ω and I_ω are the frequency-dependent voltage and current respectively (Armstrong and Henderson, 1972 and Singh et al., 2015).

Equivalent Circuit-based Analysis

In a simple scenario, the interface can be described using an equivalence circuit, commonly known as the Randles circuit. An equivalent circuit (EC) as shown in Fig. 5 is used to fit the experimental results. Figure 5 displays that a simple EC comprises of solution resistance (R_s), double-layer capacitance (C_{dl}), charge transfer resistance (R_{ct}), and Wargburg impedance (W). Besides these, inductors are also important units of EC, there is more than one way by which these components can be arranged in an EC depending on the nature of the redox processes occurring at the electrode-electrolyte interface. The simplest of them is the Randles circuit. The difference between the experimental and simulated values should be as small as possible for a clear understanding of the processes occurring at the electrode surface (Nikoo et al., 2017).

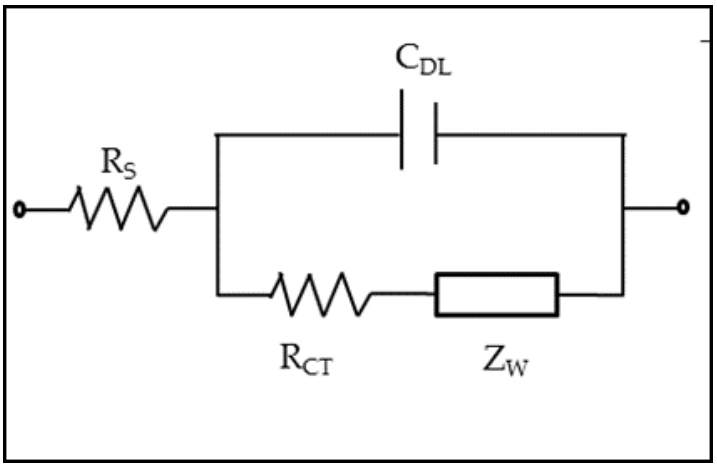

Fig. 5: Randles circuit for EIS (VanderNoot and Abrahams 1998).

The Nyquist and Bode plots are the two most convenient ways to treat impedance data.

a) Nyquist Plot

Fig. 6 shows Nyquist plot, in which imaginary component of the impedance is plotted on y-axis and real component on x- axis. In an Nquist plot, the impedance that appears at higher frequency represents solution resistance while charge transfer resistance is estimated from lower frequency region. A small value of charge transfer resistance is an indication of facile transfer of electrons (fast kinetics) at the electrode surface and vice versa.

b) Bode Plot

Bode graphs show the absolute values of impedance or phase angle vs frequency. It also delivers essentially identical information as the Nyquist plot. The Φ vs log ω in Fig. 6 indicates that the material is resistant in both high and low frequency ranges. This is confirmed with no phase shift. At intermediate frequencies, the responses grow more capacitive as the phase shift approaches 90º (Park and Yoo, 2003).

Reasons to Run EIS

Characterization of Electrochemical Systems

EIS provides extensive information about the electrical properties of electrochemical systems, assisting in the understanding of resistances, capacitances, and reaction rates.

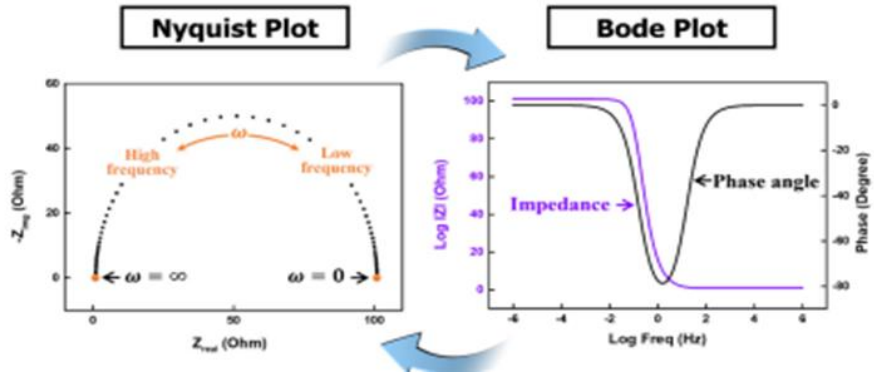

Fig. 6: Nyquist Plot and Bode plot for EIS (Birke, 1981).

Understanding Reaction Mechanisms

EIS uses impedance spectra analysis to discover and comprehend electrochemical processes such as charge transfer reactions, mass transport events, and surface changes.

Detection of Electrochemical Interfaces

EIS sensitivity allows for the detection and characterizations of events such as adsorption desorption, and corrosion at electrode interfaces.

Quality Control and Process Optimization

EIS helps to ensure consistency and dependability throughout the fabrication of electrochemical devices and coatings.

Interdisciplinary Applications

EIS has applications in a variety of domains, making it an invaluable tool for researchers and practitioners working on electrochemical problems and applications.

EIS is non-destructive and non-invasive, allowing for repeated measurements without affecting system integrity, which is advantageous for fragile or sensitive systems. EIS provides key insights required for the development of novel materials and devices in areas such as chemistry, physics, and engineering.

Conclusion:

To summarize, the characterisation of nanoparticles necessitates a multidisciplinary approach using a variety of experimental approaches. X-ray diffraction (XRD) allows for structural investigation of crystalline materials, whereas scanning electron microscopy (SEM) provides information about surface morphology and composition. Thermal analysis (TA), which includes thermogravimetric analysis (TGA) and differential scanning calorimetry (DSC), yields critical information on thermal behavior and phase transitions. Electrochemical analysis techniques like cyclic voltammetry (CV) and electrochemical impedance spectroscopy (EIS) provide useful information on redox processes and interfacial phenomena. By combining these techniques, researchers can gain comprehensive insights into the properties and behavior of nanoparticles materials, facilitating understanding and enabling the development of advanced applications in fields such as materials science, energy storage, and catalysis.

REFERENCES

Hanawalt, J., Rinn, H., and Frevel, L. (1938). Chemical analysis by X-ray diffraction. *Industrial and Engineering Chemistry Analytical Edition*, 10(9), 457- 512.

Alexander, L., and Klug, H. P. (1950). Determination of crystallite size with the X-Ray spectrometer. *Journal of Applied Physics*, 21(2), 137-142.

Armstrong, R. D., and Henderson, M. (1972). The impedance of transpassive chromium. *Journal of Electroanalytical Chemistry and Interfacial Electrochemistry,* 40(1), 121-131.

Birke, R. L., Kim, M. H., and Strassfeld, M. (1981). Diagnosis of reversible, quasi-reversible, and irreversible electrode processes with differential pulse polarography. *Analytical Chemistry*, 53(6), 852-856.

Brown, M. E. (1989). Introduction to thermal analysis: techniques and applications. *Mineralogical Magazine*, 53(373), 1-207.

Bunaciu, A. A., UdriŞTioiu, E. G., and Aboul-Enein, H. Y. (2015). X-ray diffraction: instrumentation and applications. *Critical Reviews in Analytical Chemistry*, 45(4), 289-299.

Choi, W., Shin, H. C., Kim, J. M., Choi, J. Y., and Yoon, W. S. (2020). Modeling and applications of electrochemical impedance spectroscopy (EIS) for lithium-ion batteries. *Journal of Electrochemical Science and Technology*, 11(1), 1-13.

Cullity, B. D. (1956). Elements of X-ray Diffraction (pp. 81-106). Addison-Wesley Publishing.

Dinnebier, R. E., and Billinge, S. J. (2008). Powder diffraction: Theory and practice (pp. 1-19). Royal Society of Chemistry.

Ebnesajjad, S. (2010). Surface and material characterization techniques. Handbook of adhesives and surface preparation: technology, applications and manufacturing (pp. 31-48). William Andrew.

Ford, B.J., Savile, B. and Joy, D. C. (2019). Scanning electron microscope. Encyclopedia Britannica. https://www.britannica.com/technology/scanning-electron-microscope.

Gabbott, P. (2008). Principles and applications of thermal analysis (pp. 1-118). Wiley Blackwell.

Gallagher, P. K. (1998). Thermogravimetry and thermomagnetometry. Handbook of thermal analysis and calorimetry (pp. 225-278). Elsevier Science BV.

Gill, P., Moghadam, T. T., and Ranjbar, B. (2010). Differential scanning calorimetry techniques: applications in biology and nanoscience. *Journal of Biomolecular Techniques*, 21(4), 167.

Goodhew, P. J., Humphreys, J., and Beanland, R. (2000). Electron microscopy and analysis (pp. 20-37). CRC press.

Holzwarth, U., and Gibson, N. (2011). The Scherrer equation versus the 'Debye-Scherrer equation'. *Nature Nanotechnology*, 6(9), 534-534.

Huang, J., Li, Z., Liaw, B. Y., and Zhang, J. (2016). Graphical analysis of electrochemical impedance spectroscopy data in Bode and Nyquist representations. *Journal of Power Sources,* 309, 82-98.

Isaev, V. A., Grishenkova, O. V., and Zaykov, Y. P. (2018). Theory of cyclic voltammetry for electrochemical nucleation and growth. *Journal of Solid State Electrochemistry*, 22(9), 2775-2778.

Jenkins, R., and Snyder, R. L. (1996). Introduction to X-ray Powder Diffractometry (pp. 1-22). NY, John Wiley and Sons, Inc.

Muniz, F. T. L., Miranda, M. A. R., Morilla dos Santos, C., and Sasaki, J. M. (2016). The Scherrer equation and the dynamical theory of X-ray diffraction. Acta Crystallographica Section A: Foundations and Advances, 72(3), 385-390.

Nikoo, M., Sadowski, Ł., and Nikoo, M. (2017). Prediction of the corrosion current density in reinforced concrete using a self-organizing feature map. *Coatings*, 7(10), 160.

Park, S. M., and Yoo, J. S. (2003). Peer reviewed: EIS for better electrochemical measurements. *Analytical Chemistry*, 75(21), 455-461.

Parlouer, P. L. (2013). Thermal analysis and calorimetry techniques for catalytic investigations. Calorimetry and thermal methods in catalysis (pp. 51-101). Springer, Berlin, Heidelberg.

Pirozzi, N. M., Kuipers, J., and Giepmans, B. N. (2021). Sample preparation for energy dispersive X-ray imaging of biological tissues. *Methods in Cell Biology*, 162, 29-114.

Singh, R. K., Devivaraprasad, R., Kar, T., Chakraborty, A., and Neergat, M. (2015). Electrochemical impedance spectroscopy of oxygen reduction reaction (ORR) in a rotating disk electrode configuration: effect of ionomer content and carbon-support. *Journal of The Electrochemical Society*, 162(6), 489-498.

Ul-Hamid, A. (2018). A beginners' guide to scanning electron microscopy (pp. 1-14). Springer.

VanderNoot, T. J., and Abrahams, I. (1998). The use of genetic algorithms in the non-linear regression of immittance data. *Journal of Electroanalytical Chemistry*, 448(1), 17-23.

Vernon-Parry, K. D. (2000). Scanning electron microscopy: an introduction. *III-Vs Review*, 13(4), 40-44.

Zahn, R., Coullerez, G., Vörös, J., and Zambelli, T. (2012). Effect of polyelectrolyte interdiffusion on electron transport in redox-active polyelectrolyte multilayers. *Journal of Materials Chemistry*, 22(22), 11073-11078.

Zhao, S., Wei, G. W., and Xiang, Y. (2005). DSC analysis of free-edged beams by an iteratively matched boundary method. *Journal of Sound and Vibration*, 284(1-2), 487-493